European Journal of Technique

journal homepage: https://dergipark.org.tr/en/pub/ejt

Vol.12, No.2, 2022

PLL-Less Active/Reactive Power Control of Photovoltaic Energy Source with Applying *pq*-Theory in Single-Phase Grid System

Mehmet Büyük[1*]

[1*]Adıyaman University, Electrical-Electronics Engineering Department, 02040, Adıyaman, Türkiye (e-mail:mbuyuk@adiyaman.edu.tr).

ARTICLE INFO

Received: Jun., 10. 2022
Revised: Jul., 22. 2022
Accepted: Oct, 05. 2022

Keywords:
Renewable energy systems
Grid-connected inverter
PLL-less control
pq-theory
Reactive power support

Corresponding author: *Mehmet Büyük*

ISSN: *2536-5010* | e-ISSN: *2536-5134*

DOI: https://doi.org/10.36222/ejt.1129083

ABSTRACT

Converter systems are applied to manage active/reactive power control of photovoltaic (PV) source during integration with the electric grid system. The control algorithm of the conventional converter system consists of a reference generation unit, a dc-link voltage control loop, two power control loops and a phase lock loop (PLL) system. PLL unit is used to lock in phase angle of the electric grid, and to perform the coordinate transformation for calculations of the active/reactive powers. However, the control algorithm has a slow dynamic response because of utilisation of a PLL structure. In addition, additional complex mathematical computations are required with the use of a PLL algorithm. Furthermore, the interaction of the PLL and the power control loops may lead power oscillation problems under weak grid, and also result in instability of the PV system. In this study, to avoid the aforementioned issues and to enhance the power flow capability of the grid-connected PV panels, a PLL-less control algorithm in *pq*-theory is studied for the active/reactive power management and the grid synchronization. In addition, the mathematical formulations of the current control algorithm are presented in detail. To show the effectiveness of the PLL-less controller, a PV system model with using real PV panel groups is designed and constructed in a simulation environment. The proposed control method is tested under various operation cases such as dynamic environmental conditions, reactive power support and voltage variations. The proposed method shows efficient performance under applications of the different operation situations.

1. INTRODUCTION

Due to decreasing fossil fuels and rising demand for electrical energy, the use of renewable energy sources (RESs) in the electric grid system has increased dramatically around the world recently. Expanding the use of renewable energy sources is critical for supplying electricity and meeting future demand [1]. Once the RESs are used in expanded points in the electric grid system, they are referred to as distributed energy systems (DESs). With a growing demand for clean energy resources like as photovoltaic (PV), wind turbine (WT), and fuel cell technology, the word DESs is becoming increasingly often used (FC) [2]. PV systems have become into prominent among DESs owing to their wide advantages such as cheaper, robustness and easy installation [3]. In addition, PV system application has the potential to improve the electric network in terms of energy supply, power control, and system stability in this way. [4, 5]. Furthermore, by reducing the amount of power flowing through the distribution system, the electric grid's safety can be enhanced [1]. Moreover, the application of PV sources has contributed for efficient power utilization requirements in electric network system, particularly in low-voltage level applications [6, 7].

In electric grid system, the integration of PV units has been implemented in single-phase or three-phase configurations for the grid connection. A PV power structure needs proper power electronic converters for suitable power conversion during coupling with the electric grid [8, 9]. Two different stages, namely dc-dc converter and dc-ac converter, are usually applied for grid-connected RESs to control power flow and to provide a high quality power for the electric grid [10]. The main objective of the dc-dc converter is to ensure tracking of maximum power point (MPP) with an appropriate dc-link voltage level for the dc-ac converter [11]. Differently, a dual controller can be applied in PV system to achieve operation under mode change [12]. And the dc-ac converter is used to convert the dc power into ac power, and it is the key technology for the integration of PV panels into the utility grid. A convenient control algorithm is requested for the dc-ac inverter in order to satisfy the power management and reliable operation during the electric grid connection [13, 14]. Thus, the controller of the inverter should meet the requirements of the electric grid interconnection determined via regional and international standards.

In grid-connected PV system applications, control mechanism is used to satisfy the control of the dc-ac inverter,

and thus ensures the adjustment of the amount of the active and reactive powers supplied by the inverter system [15, 16]. The control algorithm of the dc-ac inverter usually consists of a dc-link voltage controller, a current/power controller, a reference generation unit and a phase lock loop (PLL) system. However, the main disadvantage of the inverter control algorithm is a slow dynamic tracking of the grid voltage due to using a PLL algorithm [17]. The application of the PLL requires extra heavy mathematical computations. Furthermore, some harmonic issues may occur under weak electric network due to the interaction of the PLL algorithm with the current/power control loop. This interaction may also lead to instability of the overall system [18]. Therefore, the calculation cost of the control algorithm can be lowered, and system stability can be improved during weak grid operation, by eliminating the necessity for the PLL system [19].

In literature, several PLL-less control algorithms are offered for the grid-connected PV systems to prevent the drawbacks of PLL application in the control loop. PLL-less control methods are examined for the single-phase [20, 21] and three-phase [22, 23] grid connected PV systems. Despite the fact that there have been some studies on PLL-less control algorithms for three-phase systems, the majority of researchers/academicians have focused on single-phase DES architectures. In [20], a PLL-less control system is suggested for a single stage grid-connected PV system. The rms quantity of the electric network voltage is needed to obtain the sinus and cosine functions for the coordinate transformation. However, when calculating the grid voltage rms value, there is a signal period delay, which influences the response time. In [24] and [25], different PLL-less control algorithm is suggested for using in active and reactive power management in PV source. However, an extra peak detector is applied to perform the synchronization capability. On the other hand, Khan et al. propose a dual loop controller in parallel without PLL need. [26, 27], in which two modulation parameters are acquired as a results of the proposed technique. Besides, the modulation parameters are summed to compute the reference modulation value, which brings about complicated switching modulation. Different from previous methods, advanced PLL-less control methods are reported by applying sliding mode control in Ref. [28] and nonlinear input-to-state-stability theory in Ref. [29]. In Ref. [30], a vector control based PLL-less method is applied for PV system, in which d-q vectors are used in control algorithm. However, aforementioned algorithms require more complex mathematical calculations to ensure PLL-less controller.

In this paper, a pq-theory control method without need of PLL algorithm is proposed for a single-phase grid-connected PV system to supply active/reactive power and to synchronize the electrical grid under a kind of operation cases. In this context, orthogonal signals of voltage and current signals are generated for active and reactive power calculation. Second-order generalized integrator (SOGI) function is preferred in this study to get the orthogonal components. The mathematical formulation of the SOGI function is provided in s-domain. To verify the effectiveness of the PLL-less control method, a single-phase grid-connected PV model has been designed and constructed in a simulation program environment. The proposed controller is tested under dynamic conditions such as temperature and irradiance changes. In addition, a reactive support case is examined to observe the response of the proposed technique. Moreover, the effectiveness of the proposed control is also tested under variations of the grid voltage. The proposed method has a remarkable response under voltage variations such as voltage sag and swell.

The rest of the paper is as follows; In Section 2, the configuration and design of the proposed system are described in detail. In Section 3, the PLL-less approach in pq-theory for the single-phase grid-tied PV system is presented. In addition, a comparison with the existing methods for single-phase PV sources is given in this section. The verification and assessment of the PLL-less method under various case studies are introduced in Section 4. And the conclusions are presented in Section “Conclusions”.

2. CONFIGURATION AND DESIGN OF THE PROPOSED SYSTEM

In this section, the power system configuration and system design of the single-phase grid-connected PV panels are conducted. By this way, the power system topology for a single-phase electrical system is illustrated. In addition, the design procedure of the proposed power system is briefly demonstrated.

2.1. Power circuit configuration of the grid-connected PV system

The block scheme of the proposed system configuration is demonstrated in Fig. 1. The proposed system is a single-phase electrical system that involves PV panel group, converter interface unit and the electric grid. PV source panels are able to supply active power for the electrical grid. Additionally, the converter system consists of a dc/dc converter and dc/ac inverter for interfacing the PV system with the electric network. Three-lag dc-dc boost converter topology is preferred in the current study to obtain lower ripple harmonic current. The boost converter controls the active power injected by PV units. On the other hand, the single-phase inverter system consists of a dc-link capacitor, an H-bridge inverter, an LCL ripple filter and a control algorithm. The dc-link capacitor maintains a stable dc voltage at the dc-link bus. The inverter performs the conversion of dc voltage into ac voltage. The control algorithm satisfies the control of active/reactive powers, dc voltage regulation and synchronization to the electrical grid. Besides, the LCL filter is used to interface the inverter to the electrical grid and to effectively reduce the high frequency ripple harmonics generated from the inverter.

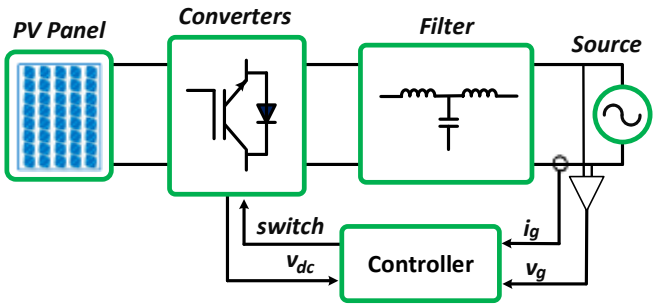

Figure 1. Power system structure of the single-phase grid-tied PV source

In the grid-connected PV systems, the conversion of the electrical energy and the control of the active/reactive powers are performed via the inverter system. The supplied active/reactive power amount is obtained by specifying the injected current amplitude and the phase angle with respect to the network phase voltage. The phase voltage and the supplied current from the inverter system are determined by equations (1) and (2).

$$v_g(t) = V_g \cos(wt + \emptyset_v) \quad (1)$$

$$i_g(t) = I_g \cos(wt + \emptyset_i) \quad (2)$$

where, V_g and I_g define the magnitudes of the electrical network voltage and the grid-side current of the inverter. Besides, $\emptyset_v$ and $\emptyset_i$ are the phase angles of the grid voltage and the current used for synchronization and power control.

The phase voltage magnitude and angle value are dependent to the electrical grid situations. Besides, the grid-side current amplitude and phase angle are calculated with the active power produced by PV energy amount and the reference reactive power value. The relationship of the injected active/reactive powers with the grid voltage, current and phase angles are given as Eq. (3). The voltage phase angle is usually selected as the reference angle during synchronization.

$$\left.\begin{aligned} P_{inj} &= \frac{1}{2}(V_g I_g \cos(\emptyset_v - \emptyset_i)) \\ Q_{inj} &= \frac{1}{2}(V_g I_g \sin(\emptyset_v - \emptyset_i)) \end{aligned}\right\} \quad (3)$$

where, the supplied active power is approximately equal to the power of PV source, ($P_{inj} \approx P_{pv}$). In addition, the reactive power is chosen according to the reference active power, in which the system controller decides according to power factor value, ($Q_{inj} = Q_{ref}$).

2.2. Design procedure of power circuit

In the grid-connected PV system, the design of the overall system consists of the design two systems: one is the design of PV panels with interfacing system, and the other is the inverter system design. Since the first one is out of scope of this study, the design of the inverter system is only presented in this section.

In this study, a single-phase inverter system is applied for interfacing PV units with the electrical grid. The overall design of the single-phase inverter system comprises the designs of the H-bridge inverter, the dc-link capacitor and the output LCL filter. The design of the inverter is related to the selection of the switching components (i.e. MOSFETs or IGBTs). The selection of the components is mainly decided according to the rated values of the system operating voltage, current and frequency variables. Thus, considering these parameters, the optimal components could be chosen from the electronic market.

On the other side, the dc-link capacitor is selected in terms of the system power, switching frequency, dc-link voltage and voltage ripple [31]. Thus, the dc-link capacitance is chosen according to the Eq. (4).

$$C_{dc} \geq \frac{0.15 S_N}{V_{dc} \Delta V_{dc} f_s} \quad (4)$$

where, S_N is the rated power of the inverter system. V_{dc} and ΔV_{dc} are the rated dc-link voltage and its allowable ripple ratio. f_s is the modulation frequency of the inverter.

The other design of the inverter system is the output LCL filter. This filter type includes two inductors and one capacitor. In design of the filter, the components are chosen by taking account the modulation index, the injected current ripple, the resonance frequency of the filter, voltage drop caused by inductances and power factor ratio in addition to the rated current and voltage values [2, 32]. The inductances/capacitance values are obtained by using the equations (5-7).

$$C_f \leq \frac{0.05 S_N}{3 w_0 V_N^2} \quad (5)$$

$$\frac{2V_{dc}(1 - m_i)m_i}{4 I_N \Delta I_{max} f_s} \leq L_1 + L_2 \leq \frac{3 V_g^2}{10 w_0 S_N} \quad (6)$$

$$L_2 = r L_1 \quad (7)$$

where, I_N and ΔI_{max} are the rated current value and its maximum ripple ratio. m_i determines the modulation index. Besides r is the split ratio between the inverter-side inductance (L_1) and the grid-side inductance (L_2). The split ratio is selected to be equal or higher than 1 [32].

In addition to these parameters, the selected values must satisfy the resonance frequency (w_r) range as (8). The resonance frequency should be higher than 10 times of the grid frequency and lower than half of the switching frequency.

$$10 w_0 \leq w_r \leq 0.5 w_s \quad (8)$$

where, $w_r = \sqrt{\frac{L_1 + L_2}{L_1 L_2 C_f}}$

According to the design criteria mentioned above, the entire system parameters are given in Table 1. The frequency response of the LCL filter according to the parameters in Table 1 is illustrated in Fig. 2. It can be seen the resonance frequency is dropped in the range determined in Eq. (8).

TABLE I
THE SYSTEM PARAMETERS OF THE PROPOSED SYSTEM

Electrical Grid	
Grid voltage (V_g)	311 V
Grid frequency (w_0)	100π rad/s
Inverter System	
Rated power (S_N)	5 kVA
DC-link voltage (V_{dc})	380 V
DC-link capacitor (C_{dc})	2.4 mF
Switching frequency (f_s)	7.5 kHz
LCL-filter	L_1 = 1 mH L_2 = 1 mH C_f = 50 µF

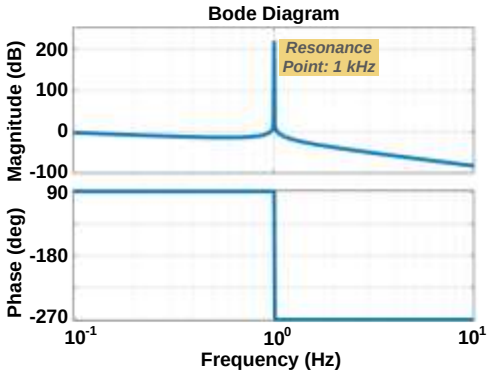

Figure 2. Frequency response of LCL filter applied in the system

3. PLL-LESS CONTROL METHODOLOGY IN PQ-THEORY

In this section, the PLL-less control mechanism in pq-theory is introduced for application in single-phase grid-connected PV sources. Moreover, to show the advantages of the proposed method, an illustrative table of the current literature is presented at the end of the section.

Figure 3 shows the detailed electrical circuit model of the single-phase grid-connected PV system. A three-lag dc-dc boost converter is applied between the PV panels and the inverter. Moreover, the details for the single-phase inverter

system are conducted in the previous section. Thus, the PLL-less control scheme in pq-theory for the inverter system is presented in detail in this section. The control algorithm of the inverter system is shown in Fig. 4. The control algorithm includes only three controller units; a dc-link controller and active/reactive power controllers. A PI controller is exploited for both the dc-link controller and power controllers.

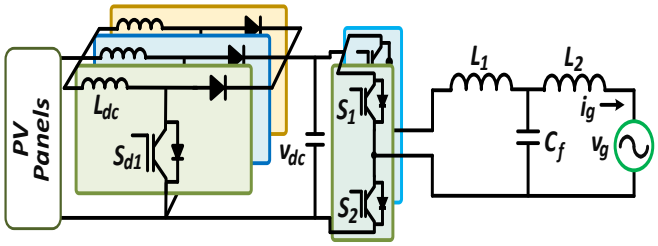

Figure 3. The detailed circuit diagram of the single-phase grid-connected PV system topology

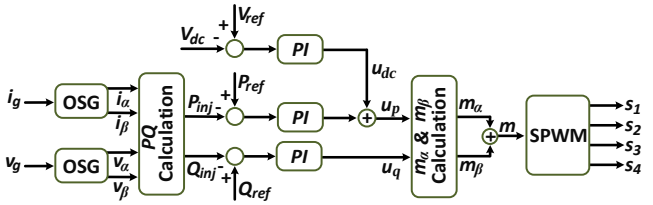

Figure 4. The control mechanism of the single-phase grid-connected PV source

The first step in control mechanism is to obtained orthogonal signals of voltage and current signals. Orthogonal signal generator (OSG) is applied for voltage and current to get the orthogonal signals. The OSG is a type of band-pass filter. The orthogonal signals (X_α-X_β) in s-domain are acquired as Eqs. (9) and (10).

$$X_\alpha(s) = \frac{kw_0 s}{s^2 + kw_0 s + {w_0}^2} X_g(s) \tag{9}$$

$$X_\beta(s) = \frac{k{w_0}^2}{s^2 + kw_0 s + {w_0}^2} X_g(s) \tag{10}$$

where, X implies the voltage signal V or current signal I. k is the coefficient for the controlling the response time and bandwidth. A phase delay is produced via the band-pass filter to generate the β component of voltage or current [9]. The frequency response of transfer functions for the α and β components are plotted in Fig. 5. It is obvious that the both signals are unity at 50 Hz frequency. Besides, α component has zero phase delay during the phase delay of β component is 90 degree. The waveforms of the generated α and β components of the signal X are illustrated in Fig. 6. As shown in Fig. 6, the grid signal X_g equals to X_α signal, and V_β signal is obtained by a 90^o phase delay to the α component.

After generation of the orthogonal signals of the voltage and current components, the active and reactive power are computed for power control. The injected active and reactive powers by the inverter system are obtained by the orthogonal signals as Eqs. (11-12).

$$P_{inj} = {}^1\!/_2\,(v_\alpha i_\alpha + v_\beta i_\beta) \tag{11}$$

$$Q_{inj} = {}^1\!/_2\,(v_\beta i_\alpha - v_\alpha i_\beta) \tag{12}$$

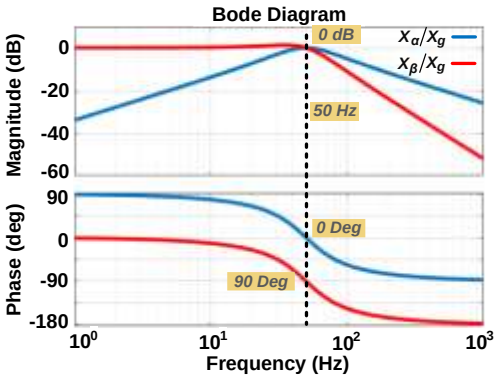

Figure 5. The frequency responses of the transfer functions for α and β components

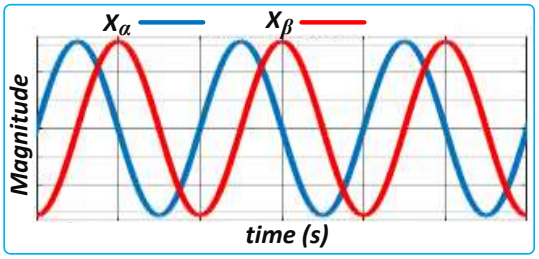

Figure 6. The waveforms of α and β components generated from OSG function

To control the power amount, the injected powers are extracted from the reference active and reactive power values to obtain power errors. Then, the error signals are curbed via the PI controllers for generating active and reactive reference components. The reference components are obtained as Eqs. (13-14).

$$u_p = k_p P_{err} + k_i \int P_{err} dt + u_{dc} \tag{13}$$

$$u_q = k_p Q_{err} + k_i \int Q_{err} dt \tag{14}$$

where, $P_{err} = P_{ref} - P_{inj}$ and $Q_{err} = Q_{ref} - Q_{inj}$. k_p and k_i are the PI parameters for the power controllers. P_{ref} is determined via MPPT controller and Q_{ref} is defined according to reactive power requirement by the electric grid. u_{dc} is the reference signal for the dc-link voltage fluctuations, in which it is determined as Eq. (15).

$$u_{dc} = k_{p,dc}(V_{ref} - V_{dc}) + k_{i,dc} \int (V_{ref} - V_{dc}) dt \tag{15}$$

where, $k_{p,dc}$ and $k_{i,dc}$ are proportional and integrator coefficients, respectively.

After that, the orthogonal modulation indices (m_α and m_β) can be derived by the Eqs. (16-17) as follows.

$$m_\alpha = \frac{(u_p + v_{\alpha\beta}^2)}{v_{dc}} v_\alpha + \frac{u_q}{v_{dc}} v_\beta \tag{16}$$

$$m_\beta = \frac{(u_p + v_{\alpha\beta}^2)}{v_{dc}} v_\beta - \frac{u_q}{v_{dc}} v_\alpha \tag{17}$$

The actual modulation signal is obtained via addition of the both orthogonal indices given in Eqs. (16) and (17), $m = m_\alpha + m_\beta$. v_{dc} and $v_{\alpha\beta}^2$ are the mean of the dc-link voltage and the square of the grid voltage amplitude, respectively. $v_{\alpha\beta}^2$ is calculated as follows.

$$v_{\alpha\beta}^2 = v_\alpha^2 + v_\beta^2 \quad (18)$$

The modulation signal is then compared with a triangle wave having 7.5 kHz frequency. The switches S_1 and S_4 are triggered once the reference is higher, and S_2 and S_3 are switched vice versa.

In addition, sinus and cosine function can be generated to apply for signal transformations. This can be achieved by dividing α and β components to the voltage amplitude as given in (19).

$$cos\theta = v_\alpha / v_{\alpha\beta}$$
$$sin\theta = v_\beta / v_{\alpha\beta} \quad (19)$$

Furthermore, to illustrate the benefits of the proposed control algorithm, a comparison of the single-phase grid-connected PV systems is presented in Table 2 through investigating several methods in literature in terms of the reference generation frame, PLL usage, and number and types of controllers.

TABLE II
A COMPARISON OF THE PROPOSED SYSTEM WITH THE SINGLE-PHASE GRID-CONNECTED INVERTER SYSTEMS

Ref. No	Reference Generation	PLL Usage	# of Controller			Modulation Method
			P/PI	PR	Others	
[33]	pq-theory	Yes	3	1	-	SPWM
[7]	pq-theory	Yes	1	2	-	SPWM
[34]	SRF	NA	3	-	-	SPWM
[35]	pq-theory	Yes	1	-	2 MPC	SPWM
[26]	SRF	No	3	-	-	SPWM
[36]	SRF	Yes	2	-	-	Hysteresis
[37]	SRF	Yes	2	-	-	SPWM
[38]	pq-theory	Yes	2	-	-	Hysteresis
Current Study	pq-theory	No	2	-	-	SPWM

(NA: Not Available, SRF: Synchronous Reference Frame, MPC: Model Predictive Control)

4. CASE STUDIES AND ASSESSMENT

In this section, the proposed control algorithm scheme is evaluated for a single-phase grid-tied PV units under various case studies. To examine the effectiveness of the proposed method, a grid-connected PV system is designed and constructed in a simulation environment. The rated power of the PV panels is constructed to apply a maximum 4.27 kW under optimal environmental situations. The PV modules are selected from SunPower manufacturer with SPR-305E-WHT-D model code, where each panel has 305 W maximum power generation rating. In accordance, seven series with two parallel string array is connected to acquire the rated power from the PV units.

The control algorithm is firstly examined under different voltage conditions, as illustrated in Fig. 7, in order to demonstrate the capability of the proposed method for the generation of the sinus and cosine functions. In the figure, the waveforms of the grid voltage, sinus function and cosine function are shown. A voltage sag and a voltage swell cases are constituted to examine the response of the proposed technique. The grid voltage drops to 0.7 pu from 1 pu between 1.1s and 1.2s. And it increases to 1.2 pu from 1 pu between 1.3s and 1.4s. Besides, it is unity at the other time intervals. It can be seen from the figure that the cosine and sinus functions are not affected during the voltage sag and swell cases.

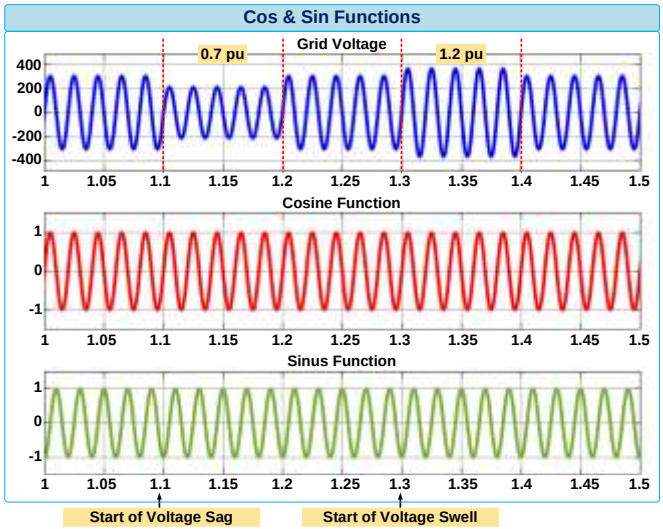

Figure 7. Generation of sinus and cosine functions under voltage sag and swell conditions

The proposed control algorithm with the designed system is investigated and verified under three different cases: (1) Dynamic operation conditions, (2) Reactive power support and (3) Voltage sag and swell.

4.1. Case 1: Dynamic operation conditions

The proposed method is investigated under a dynamic operation case in order to provide reliable and efficient operation of the proposed method for the grid-connected PV system. By this way, the proposed method is investigated under different temperature and irradiance values. Moreover, the proposed algorithm can be applied for other distributed sources such as FC unit under temperature changes and wind energy under various wind speed values.

Figure 8 shows the changes in the temperature and irradiance between 0.5s and 3s time intervals for verifying the proposed control method in dynamic operation condition. It is clear from the figure a temperature change is applied between 1s-2s time interval by increasing to 31 ^{0}C from 25 ^{0}C. In addition, the irradiance varies from 1000 W/m^2 to 600 W/m^2.

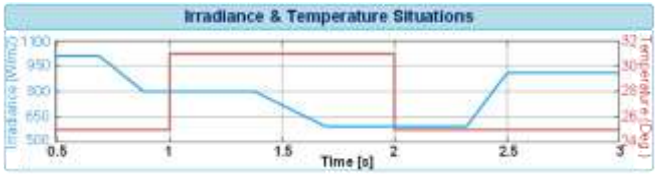

Figure 8. Irradiance and temperature situations for dynamic operation case

The response of the proposed method under the temperature and irradiance variations in Fig. 8 is demonstrated in Fig. 9. The grid voltage, grid current, dc-link voltage and the injected active power are given in Fig. 9. It can be seen that the grid current, the dc-link voltage and the injected active power have smooth responses with the proposed method under the dynamic temperature and irradiance changes. The dc-link voltage has almost 2-3 V oscillation during the condition changes. Besides, the injected current and active power have effective transient responses under the dynamic operation case.

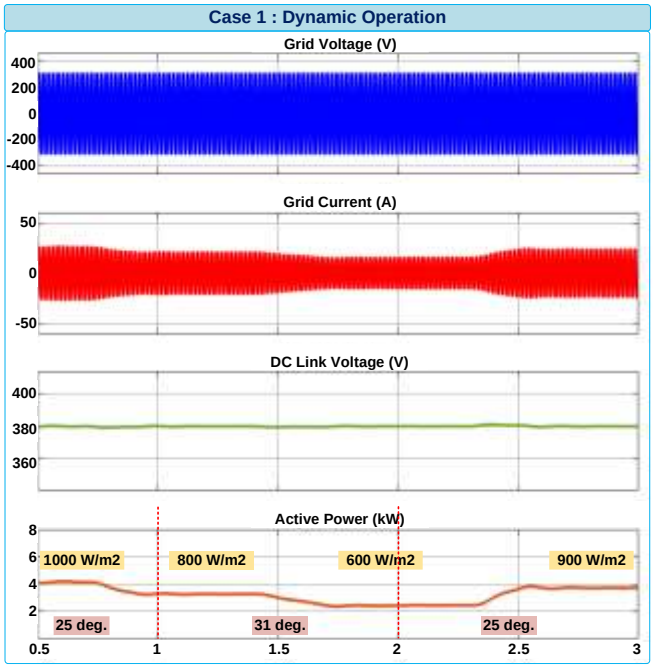

Figure 9. Response of the proposed method under changes of irradiance and temperature

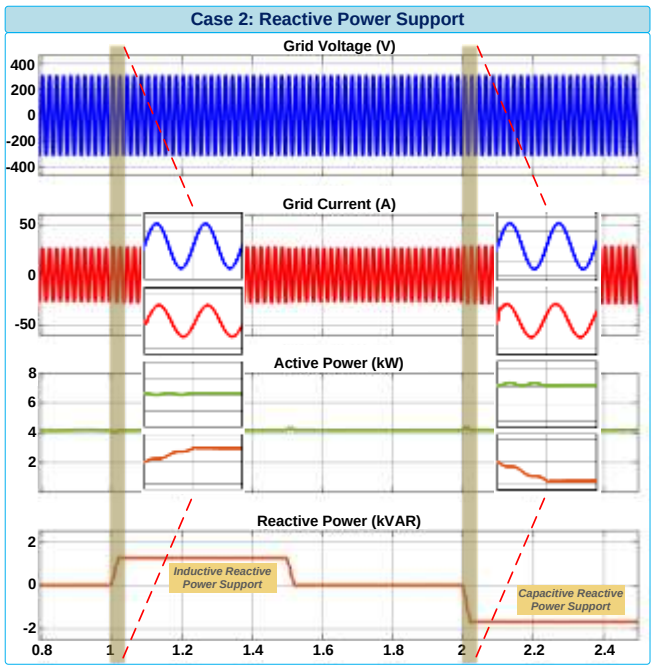

Figure 10. Injection of inductive and capacitive reactive powers to support the electrical grid

4.2. Case 2: Reactive power support

The proposed control approach is also examined by consideration of a reactive power support operation case. In this context, both capacitive reactive power and inductive reactive power support cases are performed with the proposed method. The injection of inductive reactive power and capacitive reactive power cases to support the electrical grid is indicated in Fig. 10. In the figure, the grid voltage, the grid current, the active power and the reactive power are presented. The inductive reactive power support is performed between 1s-1.5s time intervals by 30 % rating of the injected active power. Besides, a capacitive power support of forty percent of the injected active power is provided at 2s-2.5s time interval. It is obvious that the proposed method has a remarkable performance during both inductive and capacitive reactive power support events.

4.3. Case 3: Voltage sag/swell situations

In order to demonstrate the robustness of the proposed control algorithm, both sag and swell conditions of the grid voltage are evaluated in this case via varying the grid voltage amplitude. Figure 11 illustrates the waveforms of the grid voltage, the grid current, the dc-link voltage and the injected active power for both voltage sag and voltage swell situations.

The voltage sag and the voltage swell are performed by 30 % and 20 %, respectively. The voltage sag case starts at 1.1s, and lasts for five periods, as shown in Fig. 11 (a). It is clear that the proposed controller ensures a good stability performance during the occurrence of the voltage sag. The injected power is set to its stable condition at 0.06s. Moreover, the dc-link voltage has low voltage oscillation (almost 5 V), once the voltage sag occurs.

On the other side, the voltage swell case is performed at 1.3s, and similar to the voltage sag, it continues five periods, as demonstrated in Fig. 11 (b). The proposed control algorithm also shows efficient response under the voltage swell. In this case, the injected power is set to its stable situation at 0.08s. Furthermore, almost 4V oscillation is observed when the voltage amplitude arises.

5. CONCLUSIONS

In this paper, a PLL-less control algorithm in pq-theory is performed for single-phase grid-connected PV system. The PLL usage is not required with the control method in the current study. Thus, the calculation complexity of the PLL application is avoided in this study, which results in low computation burden. In addition, the instabilities that may arise from the usage of a PLL are prevented by this method. The mathematical background of the PLL-less control mechanism in pq-theory is introduced in detail. In the current controller scheme, orthogonal signals of the grid voltage and inverter current are generated by SOGI function to obtain injected powers and then calculate modulation indices. Moreover, only two controllers without dependence on a PLL application are needed in the proposed control technique.

To observe the ability of the control technique in this study, a single-phase grid-connected PV system is designed and built in the simulation environment. The performance of the control scheme in the generation of alpha and beta functions is firstly validated under weak grid operation such as voltage sag and voltage swell conditions. It is shown that the both functions do not have any impact from the occurrences of the voltage sag and swell. The control scheme is also tested for three difference scenario cases in the constructed simulation model. These cases consist of the conditions of a dynamic operation, reactive power support and voltage sag/swell, respectively. The proposed method is tested under %30 voltage sag and %20 voltage swell situations. In addition, a reactive power support with 30 percentage of the active power is supplied both for inductive and capacitive cases. The robustness and effective performance of the proposed method are verified for applications of the different temperature and irradiance values for dynamic operation case, inductive and capacitive reactive power supports in the second case, and occurrences of 30 % voltage sag and 20 % voltage swell in the third case.

 ISSN 2536-5010 | **e-ISSN** 2536-5134 https://dergipark.org.tr/en/pub/ejt

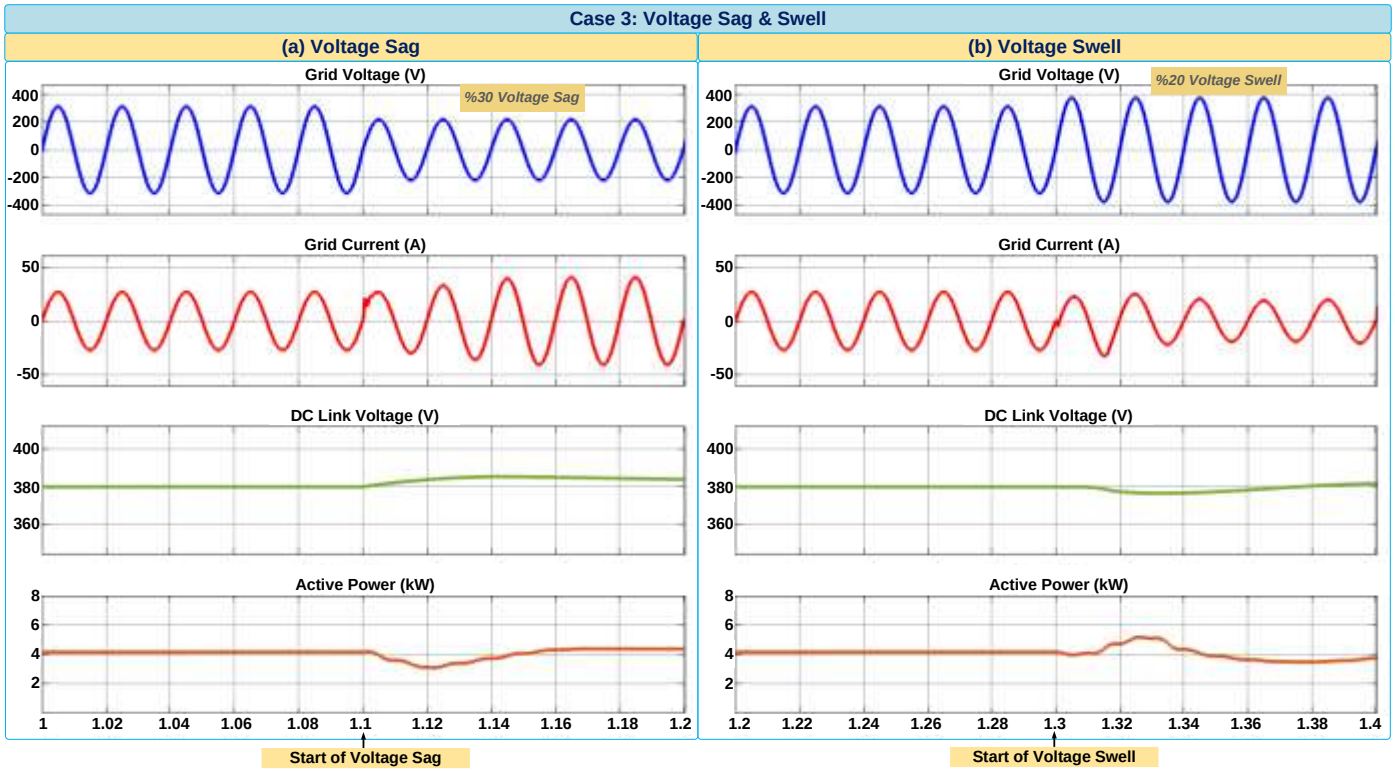

Figure 11. The response of the proposed method under (a) voltage sag and (b) voltage swell cases

REFERENCES

[1] R. Sharma and S. Mishra, "Dynamic Power Management and Control of a PV PEM Fuel-Cell-Based Standalone ac/dc Microgrid Using Hybrid Energy Storage," *IEEE Transactions on Industry Applications*, vol. PP, pp. 1-1, 09/22 2017.

[2] M. Büyük, A. Tan, M. Tümay, and K. Ç. Bayındır, "Topologies, generalized designs, passive and active damping methods of switching ripple filters for voltage source inverter: A comprehensive review," *Renewable and Sustainable Energy Reviews*, vol. 62, pp. 46-69, 2016/09/01/ 2016.

[3] K. Brecl, J. Ascencio-Vásquez, and M. Topič, "Performance of PV systems in Slovenia with the help of typical daily profiles and automatic detection of orientation and inclination angles," *Solar Energy*, vol. 236, pp. 870-878, 2022/04/01/ 2022.

[4] M. Bornapour, R.-A. Hooshmand, A. Khodabakhshian, and M. Parastegari, "Optimal coordinated scheduling of combined heat and power fuel cell, wind, and photovoltaic units in micro grids considering uncertainties," *Energy*, vol. 117, pp. 176-189, 2016/12/15/ 2016.

[5] M. A. Hannan, S. Y. Tan, A. Q. Al-Shetwi, K. P. Jern, and R. A. Begum, "Optimized controller for renewable energy sources integration into microgrid: Functions, constraints and suggestions," *Journal of Cleaner Production*, vol. 256, p. 120419, 2020/05/20/ 2020.

[6] E. Kabalcı, "Review on novel single-phase grid-connected solar inverters: Circuits and control methods," *Solar Energy*, vol. 198, pp. 247-274, 2020/03/01/ 2020.

[7] B. Liu, Z. Zhang, G. Li, D. He, Y. Chen, Z. Zhang, *et al.*, "Integration of power decoupling buffer and grid-tied photovoltaic inverter with single-inductor dual-buck topology and single-loop direct input current ripple control method," *International Journal of Electrical Power & Energy Systems*, vol. 125, p. 106423, 2021/02/01/ 2021.

[8] G. Liu, T. Caldognetto, P. Mattavelli, and P. Magnone, "Suppression of Second-Order Harmonic Current for Droop-Controlled Distributed Energy Resource Converters in DC Microgrids," *IEEE Transactions on Industrial Electronics*, vol. 67, pp. 358-368, 2020.

[9] C. Xie, K. Li, X. Zhao, J. C. Vasquez, and J. Guerrero, *Reduced Order Generalized Integrators with Phase Compensation for Three-Phase Active Power Filter*, 2017.

[10] P. Verma, T. Kaur, and R. Kaur, "Power control strategy of an integrated PV system for active power reserve under dynamic operating conditions," *Sustainable Energy Technologies and Assessments*, vol. 45, p. 101066, 2021/06/01/ 2021.

[11] J. P. Roselyn, C. P. Chandran, C. Nithya, D. Devaraj, R. Venkatesan, V. Gopal, *et al.*, "Design and implementation of fuzzy logic based modified real-reactive power control of inverter for low voltage ride through enhancement in grid connected solar PV system," *Control Engineering Practice*, vol. 101, p. 104494, 2020/08/01/ 2020.

[12] Y. Wang, B. Ren, and S. Liyanage, "Unified control scheme for a dual-stage grid-connected PV system with mode change," *Solar Energy*, vol. 239, pp. 88-101, 2022/06/01/ 2022.

[13] D. Çelik and M. E. Meral, "A novel control strategy for grid connected distributed generation system to maximize power delivery capability," *Energy*, vol. 186, p. 115850, 2019/11/01/ 2019.

[14] M. M. Savrun and M. İnci, "Adaptive neuro-fuzzy inference system combined with genetic algorithm to improve power extraction capability in fuel cell applications," *Journal of Cleaner Production*, vol. 299, p. 126944, 2021/05/25/ 2021.

[15] S. Gu, X. Du, Y. Shi, Y. Wu, P. Sun, and H. Tai, "Power control for grid-connected converter to comply with safety operation limits during grid faults," in *2016 IEEE Energy Conversion Congress and Exposition (ECCE)*, 2016, pp. 1-5.

[16] A. Q. Al-Shetwi, M. A. Hannan, K. P. Jern, M. Mansur, and T. M. I. Mahlia, "Grid-connected renewable energy sources: Review of the recent integration requirements and control methods," *Journal of Cleaner Production*, vol. 253, p. 119831, 2020/04/20/ 2020.

[17] P. Rodríguez, A. Luna, I. Candela, R. Mujal, R. Teodorescu, and F. Blaabjerg, "Multiresonant Frequency-Locked Loop for Grid Synchronization of Power Converters Under Distorted Grid Conditions," *IEEE Transactions on Industrial Electronics*, vol. 58, pp. 127-138, 2011.

[18] B. Wen, D. Boroyevich, R. Burgos, P. Mattavelli, and Z. Shen, "Analysis of D-Q Small-Signal Impedance of Grid-Tied Inverters," *IEEE Transactions on Power Electronics*, vol. 31, pp. 675-687, 2016.

[19] Y. Gui, X. Wang, F. Blaabjerg, and D. Pan, "Control of Grid-Connected Voltage-Source Converters: The Relationship Between Direct-Power Control and Vector-Current Control," *IEEE Industrial Electronics Magazine*, vol. 13, pp. 31-40, 2019.

[20] K. M. Tsang, W. L. Chan, and X. Tang, "PLL-less single stage grid-connected photovoltaic inverter with rapid maximum power point tracking," *Solar Energy*, vol. 97, pp. 285-292, 2013/11/01/ 2013.

[21] K. S. R. Sekhar and M. A. Chaudhari, "Reactive Power Enhancement of a PLL less PV inverter for AC Micro-grids," in *2020 IEEE First International Conference on Smart Technologies for Power, Energy and Control (STPEC)*, 2020, pp. 1-6.

[22] S. Dedeoglu and G. C. Konstantopoulos, "PLL-Less Three-Phase Droop-Controlled Inverter with Inherent Current-Limiting Property," in *IECON 2019 - 45th Annual Conference of the IEEE Industrial Electronics Society*, 2019, pp. 4013-4018.

[23] P. Patel, U. Mali, and G. Patel, "PLL less strategy for grid tied inverter with different load conditions," in *2017 Third International Conference on Advances in Electrical, Electronics, Information, Communication and Bio-Informatics (AEEICB)*, 2017, pp. 251-254.

[24] X. Li and R. S. Balog, "PLL-less robust active and reactive power controller for single phase grid-connected inverter with LCL filter," in *2015 IEEE Applied Power Electronics Conference and Exposition (APEC)*, 2015, pp. 2154-2159.

[25] S. Deo, C. Jain, and B. Singh, "A PLL-Less Scheme for Single-Phase Grid Interfaced Load Compensating Solar PV Generation System," *IEEE Transactions on Industrial Informatics*, vol. 11, pp. 692-699, 2015.

[26] A. Khan, M. Hosseinzadehtaher, and M. B. Shadmand, "Single Stage PLL-less Decoupled Active and Reactive Power Control for Weak Grid Interactive Inverters," *IFAC-PapersOnLine*, vol. 53, pp. 12390-12395, 2020/01/01/ 2020.

[27] A. Khan, M. Easley, M. Hosseinzadehtaher, M. B. Shadmand, H. Abu-Rub, and P. Fajri, "PLL-less Active and Reactive Power Controller for Grid-Following Inverter," in *2020 IEEE Energy Conversion Congress and Exposition (ECCE)*, 2020, pp. 4322-4328.

[28] E. Heydari, A. Y. Varjani, and D. Diallo, "Fast terminal sliding mode control-based direct power control for single-stage single-phase PV system," *Control Engineering Practice*, vol. 104, p. 104635, 2020/11/01/ 2020.

[29] G. C. Konstantopoulos, Q. Zhong, and W. Ming, "PLL-Less Nonlinear Current-Limiting Controller for Single-Phase Grid-Tied Inverters: Design, Stability Analysis, and Operation Under Grid Faults," *IEEE Transactions on Industrial Electronics*, vol. 63, pp. 5582-5591, 2016.

[30] K. S. Raja Sekhar, M. A. Chaudhari, and T. Davi Curi Busarello, "A PLL-less Vector Control technique for the single-phase Grid connected inverters," *International Journal of Electrical Power & Energy Systems*, vol. 142, p. 108353, 2022/11/01/ 2022.

[31] R. Chen, "DC Capacitor Minimization of Single Phase Power Conversion and Applications," PhD, Michigan State University., 2016, PhD Thesis.

[32] H. Cha and T. Vu, "Comparative analysis of low-pass output filter for single-phase grid-connected Photovoltaic inverter," in *2010 Twenty-Fifth Annual IEEE Applied Power Electronics Conference and Exposition (APEC)*, 2010, pp. 1659-1665.

[33] Ö. Çelik, A. Tan, M. İnci, and A. Teke, "Improvement of energy harvesting capability in grid-connected photovoltaic micro-inverters," *Energy Sources, Part A: Recovery, Utilization, and Environmental Effects*, pp. 1-25, 04/24 2020.

[34] C. Kalavalli, P. Meenalochini, P. Selvaprasanth, and S. Syed Abdul Haq, "Dual loop control for single phase PWM inverter for distributed generation," *Materials Today: Proceedings*, vol. 45, pp. 2216-2219, 2021/01/01/ 2021.

[35] M. Talha, S. R. S. Raihan, and N. A. Rahim, "PV inverter with decoupled active and reactive power control to mitigate grid faults," *Renewable Energy*, vol. 162, pp. 877-892, 2020/12/01/ 2020.

[36] S. Roy, P. Kumar Sahu, S. Jena, and A. Kumar Acharya, "Modeling and control of DC/AC converters for photovoltaic grid-tie micro-inverter application," *Materials Today: Proceedings*, vol. 39, pp. 2027-2036, 2021/01/01/ 2021.

[37] L. Hassaine and B. Mohamed Rida, "Control technique for single phase inverter photovoltaic system connected to the grid," *Energy Reports*, vol. 6, 11/01 2019.

[38] M. İnci, "Active/reactive energy control scheme for grid-connected fuel cell system with local inductive loads," *Energy*, vol. 197, p. 117191, 2020/04/15/ 2020.

BIOGRAPHIES

Mehmet Büyük received his BSc and MSc degrees in Electrical-Electronics Engineering from Çukurova University, in 2012 and 2015. He received the PhD degree in Electrical-Electronics Engineering from Çukurova University, 2019. He is currently Researcher at the department of Electrical-Electronics Engineering, Adıyaman University. His research areas are custom power devices, power quality, vehicle-to-grid (V2G) systems and wireless power transfer.